Evaluating the Efficient Market Hypothesis by means of isoquantile surfaces and the Hurst exponent

Kristýna Ivanková[1], Ladislav Krištoufek[2], Miloslav Vošvrda[3]

Abstract. This article extends our previous work on applications of isoquantile (formerly *isobar*) surfaces to market analysis. The approach is applied to lagged returns of selected stock market indices and compared to various estimations of the Hurst exponent.

We evaluate the Efficient Market Hypothesis by means of the two aforementioned approaches for the ASPI, BET, BUX, JSX, NASDAQ, PX and S&P500 indices. The more does a time series satisfy the EMH, the closer it resembles Brownian motion. In this case isoquantile surfaces form a circle and the Hurst exponent approaches $\frac{1}{2}$.

Keywords: isoquantile, isobar, Hurst exponent, Efficient Market Hypothesis, stock market index

1 Introduction

This article applies two approaches to evaluate the Efficient Market Hypothesis for selected stock market indices. The notion of an *efficient market* was introduced in Fama [6]. We study the particular version of EMH stating that returns of efficient stock market indices follow the behaviour of Brownian motion; as for this article, closeness to this ideal will be understood as a measure of efficiency.

The first section discusses the isoquantile approach introduced in [4] (originally called the *isobar* approach). For a fixed center point and a level u, an isoquantile encloses the u-th quantile of a multi-dimensional data distribution, mapping every direction from the center to a particular distance. The term "isoquantile" is used for both the mapping and its image (a continuous surface). Since isoquantiles of varying levels u continuously cover the whole domain, points in it can be ordered by comparing the levels of their (unique) encompassing isoquantiles.

The second author of [4] focused on practical estimation of isoquantile shapes. The article [9] considers estimation of the edge of the bounded support ($u \to 1$) using nonparametric regression and [10] extends this method for unbounded support using asymptotical location and isoquantiles.

In this article, we follow the approach of [9] and limit ourselves to *homothetic* isoquantiles (i.e. isoquantiles of varying levels are assumed to be scaled copies of each other). In our prior article [8] we've formulated two isoquantile shape estimation methods (differing in the chosen coordinate system) and applied them on the PX and NASDAQ indices.

The next section discusses the Hurst exponent [7, 5, 3], a measure of fractal dimension. It's commonly used in financial analysis as an indicator of long-term persistence of time series. We've chosen four commonly used methods for its estimation: detrended fluctuation analysis, rescaled range analysis, detrending moving average and height-height correlation analysis.

The third section is concerned with an application. We discuss the means to apply the approaches to a time series, summarize the tested indices and discuss the results.

[1]Institute of Economic Studies, Faculty of Social Sciences, Charles University in Prague, Opletalova 26, 110 00, Praha 1; Institute of Information Theory and Automation, Pod Vodárenskou věží 4, 182 08, Praha 8, e-mail: kristyna.ivankova@gmail.com

[2]Institute of Economic Studies, Faculty of Social Sciences, Charles University in Prague, Opletalova 26, 110 00, Praha 1; Institute of Information Theory and Automation, Pod Vodárenskou věží 4, 182 08, Praha 8, e-mail: kristoufek@ies-prague.org

[3]Institute of Information Theory and Automation, Pod Vodárenskou věží 4, 182 08, Praha 8, e-mail: vosvrda@utia.cas.cz

2 Isoquantile surfaces

Isoquantiles require us to work in polar coordinates. Choosing the Euclidean space, the transformation of a non-zero vector $\mathbf{x} \in \mathbb{R}^d$ to generalized polar coordinates is given by

$$r = \|\mathbf{x}\|_2, \quad \theta = \frac{\mathbf{x}}{\|\mathbf{x}\|_2},$$

where $\|\mathbf{x}\|_2$ is the Euclidean norm of the vector $\mathbf{x}$. Observe that the generalized angle θ lies on S^{d-1}, the sphere of unit radius in $\mathbb{R}^d$.

We'll use the definition of isoquantile as it appears in [4], page 2: For every $u \in (0, 1)$, the u-level isoquantile is defined as a mapping of a fixed θ to the value of the inverse distribution function of the Euclidean distance from the origin: $\theta \to F^{-1}_{R\,|\,\Theta}(u)$. The name "$u$-level isoquantile" will also be used interchangeably for the surface $S_u = F^{-1}_{R\,|\,\Theta}(u)$ determined by each θ with a fixed quantile u in the inverse of the conditional distribution function $F^{-1}_{R\,|\,\Theta}$.

We'll assume our sample to originate from the random variable $X = (R, \Theta)$. Assume continuity of the marginal density $f_\Theta(\theta)$, conditional density $f_{R\,|\,\Theta}(r\,|\,\theta)$ and the conditional distribution function $F_{R\,|\,\Theta}(r\,|\,\theta)$. The distribution function is assumed to be invertible, the introduced mapping continuous and strictly positive.

A rigorous definition of the introduced ordering is as follows. Consider a sample of n independent realizations of the random variable X, e.g. $X_i = (R_i, \Theta_i)$, $1 \le i \le n$. For every i there exists an unique u_i-level isoquantile containing the point X_i. Denoting $X_{i,n}$ the realizations ordered by their respective quantile values u_i, the maximum value is given by the point $X_{n,n}$ which belongs to the upper-level isoquantile with level $\max_{1\le i\le n} u_i$.

In practice, we'll assess the 1-level isoquantile on the grounds of the *asymptotical location property* as described in [10]. For large n, the furthest points from the origin lie near the $\frac{n-1}{n}$-level isoquantile. The 1-level isoquantile is then simply the edge of the bounded support.

Isoquantile estimation is performed by the non-parametric regression of [9, 10]. For the estimation we'll assume *homotheticity* of isoquantiles. The function $v(\theta)$ corresponds to the 1-level isoquantile and unambiguously describes the shape of all isoquantiles. The distribution of $\frac{\mathbf{x}}{v(\theta)}$ is spherically symmetric.

We estimate $v(\theta)$ using radial regression:

$$w(\theta) = E(R\,|\,\Theta = \theta) = c\,v(\theta),$$

The estimate of the expected value of R given $\Theta = \theta$ describes the shape of 1-level isoquantile up to a multiplicative constant. This constant is chosen in a way that the estimated expected value shape $\hat{w}(\theta)$ contains the whole data after scaling:

$$\hat{v}(\theta) = \frac{\hat{w}(\theta)}{\hat{c}}, \quad \text{where } 1/\hat{c} = \max_{1\le i\le n} \frac{R_i}{\hat{w}(\Theta_i)}$$

For practical estimation we'll use the two parametrizations introduced in [9] (hyperspherical) and [8] (unit sphere projection). For details and rationale see our previous work [8].

To enable quantitative comparison with the methods of the following section, we're introducing a numerical measure that preserves index ordering from the previously used visual assessment. This novel market efficiency measure is computed via Fourier analysis of the estimated isoquantile shape; due to size constraints, details will be revealed in an upcoming article.

3 Hurst exponent

For comparison, we present the results for another measure frequently used as a measure of market efficiency – the Hurst exponent H. The exponent $0 < H < 1$ is a characteristic measure of long-range dependence in the time series. For $H > 0.5$, the series is persistent, i.e. following a trend; while for $H < 0.5$, the series is anti-persistent, i.e. switching more frequently than a random series does. Therefore,

a deviation from $H = 0.5$ indicates possible profitable trading as there are long-range correlations in the series. Out of many Hurst exponent estimators, we use the most popular ones for the financial series – detrended fluctuation analysis, rescaled range analysis, detrending moving average and height-height correlation analysis.

Rescaled range analysis (RS) is the most traditional of the methods, proposed by [7]. According to [14], the time series of length $2^{\upsilon_{max}}$ is divided into the sub-periods of length 2^{υ}. For each sub-period, the range R of the profile is calculated as well as the standard deviation of the increments S. The rescaled range R/S_υ, based on the average rescaled ranges for each sub-period with length υ, scales as $R/S_\upsilon \propto \upsilon^H$. In our application, we set $\upsilon_{min} = 4$ and $\upsilon_{max} = \log_2 T$.

Detrended fluctuation analysis (DFA), proposed by [13], is based on scaling of variance of the detrended series. In the procedure, the profile (cumulative return deviations from the average) of the time series of length T is divided into sub-periods of length s and for each sub-period, a linear fit $X_s(t)$ of the profile is estimated. A detrended signal $Y_s(t)$ is then constructed as $Y_s(t) = X(t) - X_s(t)$. Fluctuation $F^2_{DFA}(s)$, defined as an average mean squared error from the linear fit over all sub-periods of length s, scales as $F^2_{DFA}(s) \propto s^{2H}$ [11]. To get reasonable estimates of H, we set $s_{min} = 5$ and $s_{max} = T/5$.

Detrending moving average (DMA), proposed by [1], is based on a moving average filtering. For a set window size λ, we construct a centered moving average $\bar{X}_\lambda(t)$ for each data point $X(t)$ of the series. Similarly to DFA, fluctuations $F^2_{DMA}(\lambda)$, defined as the mean squared error of $X(t)$ from $\bar{X}_\lambda(t)$, scale as $F^2_{DMA}(\lambda) \propto \lambda^{2H}$. As the centered moving average is used, we set $\lambda_{min} = 3$ and $\lambda_{max} = 21$ with a step of 2.

Height-height correlation analysis (HHCA), proposed by [2], is based on a scaling of height-height correlation function of the series $X(t)$ with time resolution ν and $t = \nu, 2\nu, ..., \nu\lfloor\frac{T}{\nu}\rfloor$ (where $\lfloor\rfloor$ is a lower integer operator). Second-order height-height correlation function of $X(t)$ is then defined as $K_2(\tau) = \sum_{t=1}^{\lfloor T/\nu \rfloor} |X(t+\tau) - X(t)|^2 / \lfloor T/\nu \rfloor$ where time interval τ generally ranges between $\nu = \tau_{min}, \ldots, \tau_{max}$. $K_q(\tau)$ then scales as $K_q(\tau) \propto \tau^{2H}$. In the following, we set $\tau_{min} = 1$ and $\tau_{max} = 20$.

4 Evaluating the efficient market hypothesis – stock market indices

The efficient market hypothesis states that returns (closing−opening price) of market indices in efficient markets behave ideally like Brownian motion (see e.g. [12]). In practice, this assumption is violated mostly by the periodic structure (day, week, quarter, year) of agent behaviour. Further bias mostly reveals non-rational behaviour, non-zero information costs or delayed reactions. Our goal is to measure the efficiency of a market using both the isoquantile and Hurst exponent approach and to compare them.

Our data consists of weekly closing and opening prices for the past ten years (sample size around 500) obtained from the Reuters Wealth Manager service.

Firstly we'll describe the results for isoquantiles. The y-axis denotes the current value of stock market index returns, the x-axis denotes their lagged values. Under the efficient market hypothesis, the isoquantile shape for this configuration should be close to a circle (since Brownian motion is independent to itself when lagged). The results were computed for lags between one and sixteen weeks. Image 1 shows examples of various isoquantile shapes for the assessed stock market indices. Our previous work [8] contains complete depictions of 1–14-week lags for the PX and NASDAQ indices.

We've applied the methods on seven stock market indices. We'll shortly summarize them before presenting the results:

- The All Share Price Index: 241 Sri Lankan stocks of the Colombo Stock Exchange
- The BET Index: 10 Romanian stocks of the Bucharest Stock Exchange.
- The BUX Index: 13 Hungarian stocks of the Budapest Stock Exchange.
- The JSX Composite Index: 379 Indonesian stocks of the Indonesia Stock Exchange.
- The NASDAQ Composite Index is comprised of 2742 stocks of the NASDAQ Stock Market.
- The PX Index is comprised of 14 stocks of the Prague Stock Exchange (only five of which are Czech).
- S&P500: 500 stocks traded on NYSE or NASDAQ.

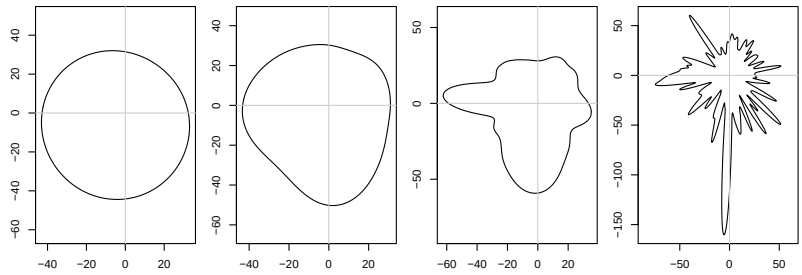

Figure 1: Examples of isobar shapes.

Isoquantile shapes for the All Share Price Index, NASDAQ Composite Index and S&P500 are very close to circles. Small deviations from the circle shape can be observed in ASPI (lags 1, 3 and 5), NASDAQ (lags 12, 13 and 16) and in S&P500 (lags 12, 13 and 16). Deviations in the 13-week lag can be explained by the expected quarterly periodicity of agent behaviour. Based on visual examination, the underlying markets of ASPI, NASDAQ and S&P500 may follow the efficient market hypothesis.

Isoquantile shapes for BET differ from circles in multiple lags (of 2, 3, 4, 11 and 13 weeks): the deviations are distinctive, which suggests short-time dependency in the data.

The isoquantile shapes of the PX Index, BUX and JSX Composite Index deviate from circles constantly: for PX it's the longer lags of 4, 7, and 9–15 weeks, for BUX it's 3 and 5–16 weeks. Isoquantiles for the JSX Composite Index don't resemble a circle for any lag. Observing a systematic deviation from independence between current values and lagged ones, we can postulate that the efficient market hypothesis doesn't apply to markets described by these indices.

The first parametrization prefers rounder shapes; isoquantiles resemble a circle more often. The second parametrization follows the data shape better.

We proceed by comparing both parametrizations with the four chosen methods of Hurst exponent estimation. Image 2 depicts both the isoquantile measures on horizontal axes plotted against Hurst exponent estimations on vertical axes. The hyperspherical isoquantile parametrization is shown in the left column, the projection parametrization in the right one. Rows subsequently depict the four Hurst exponent estimation methods in this order: rescaled range analysis (RS), detrended fluctuation analysis (DFA), detrending moving average (DMA) and height-height correlation analysis (HHCA). Each of the images additionally contains a linear fit.

The ideally effective market has isoquantile measure of zero and Hurst exponent equal to 0.5; the isoquantile measure increases with decreasing similarity to Brownian motion while the Hurst exponent approaches 1 for persistent time series. Both of these phenomena signify lower efficiency, so the measures should be positively correlated: this prediction holds for rescaled range analysis, detrended fluctuation analysis and height-height correlation analysis. The DFA method fulfills this prediction best (see e.g. [14]), followed by the RS and HHCA methods (DFA differs for NASDAQ having a lower value than S&P500, and for JSX being higher than PX). The most distant index from the linear fit is ASPI - according to the isoquantile approach it's among the most Brownian-like indices while the Hurst exponent shows pronounced persistence. This result is possibly caused by the fact that we've used short lags (1 to 16 weeks) in the isoquantile approach and the Hurst exponent measures long-term dependece. We interpret this by stating that ASPI shows dependence only in the long term. The results for DMA show almost no linear relationship between the Hurst exponent and the isobars measure. This difference is caused mainly by the low DMA estimation for JSX. Based on the construction of the methods, this indicates that JSX exhibits seasonal or cyclical behavior.

5 Conclusion

We've contrasted two approaches for studying the time dependence in time series data: the isoquantile approach (formerly called *isobar*) for short-time dependence (1–16 week lags) and the Hurst exponent for

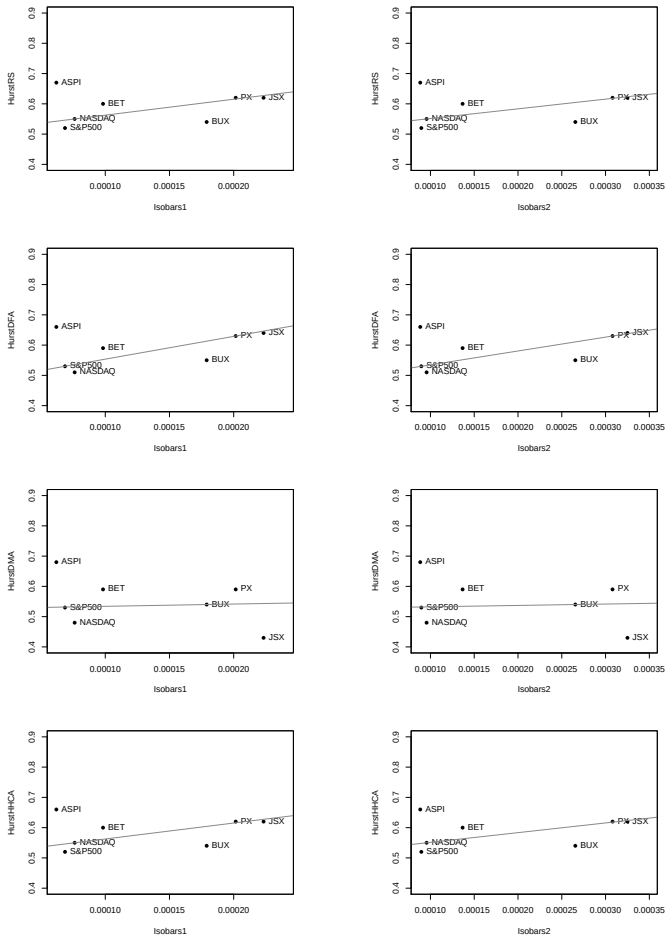

Figure 2: Isoquantile measures plotted against various Hurst exponent estimators.

long-time dependence. We've compared two parametrizations for isoquantiles (hyperspherical coordinates and unit sphere projection) and four methods for estimating the Hurst exponent (detrended fluctuation analysis, rescaled range analysis, detrending moving average and height-height correlation analysis). Using these methods we've tested the EMH for selected indices: the All Share Price Index, the NASDAQ Composite Index, S&P500, BET, PX Index, BUX and the JSX Composite Index. Since none of tested indices have shown strong anti-persistence, we've assumed a positive correlation between isoquantiles and the Hurst exponent – an assumption confirmed for three of four Hurst exponent estimation methods.

According to our results, the isoquantile approach and the Hurst exponent approach complement each other nicely, each focusing on a different dependency scale.

Acknowledgements

This work has been supported by the Czech grant agency Grant 402/09/H045, the Grant Agency of Charles University (GAUK) under project 118310 and project SVV 261 501.

References

[1] Alessio, E., Carbone, A., Castelli, G., and Frappietro, V.: Second-order moving average and scaling of stochastic time series. *European Physical Journal B* **27 (2)** (2002), 197–200.

[2] Barabasi, A.-L., Szepfalusy, P., and Vicsek, T.: Multifractal spectre of multi-affine functions. *Physica A* **178** (1991), 17–28.

[3] Cajueiro, D.O., and Tabak, B.M.: The Hurst exponent over time: testing the assertion that emerging markets are becoming more efficient. *Physica A* **336/3–4** (2004), 521–537.

[4] Delcroix, M. F., and Jacob, P.: Stability of extreme value for a multidimensional sample. *Stat. Analyse Donées* **16** (1991), 1–21.

[5] Eom, C., Oh, G., and Jung, W.: Relationship between efficiency and predictability in stock price change. *Physica A* **387/22** (2008), 5511–5517.

[6] Fama, E.: Random Walks in Stock Market Prices. *Financial Analysts Journal 5* **21** (1965), 55–59.

[7] Hurst, H.E.: Long term storage capacity of reservoirs. *Transactions of the American Society of Engineers* **116** (1951), 770–808.

[8] Ivanková, K.: Application of isobars to stock market indices. *Mathematical Methods in Economics Proceedings* (2010).

[9] Jacob, P., and Suquet, C.: Regression and edge estimation. *Stat. Prob. Lett.* **27** (1996), 11–15.

[10] Jacob, P., and Suquet, C.: Regression and asymptotical location of a multivariate sample. *Stat. Prob. Lett.* **35** (1997), 173–179.

[11] Kantelhardt, J., Zschiegner, S., Koscielny-Bunde, E., Bunde, A., Havlin, S., and Stanley, E.: Multifractal Detrended Fluctuation Analysis of Nonstationary Time Series. *Physica A* **316(1-4)** (2002), 87–114.

[12] Osborne, M. F. M.: Brownian motion in the stock market. *Operations research* **March-April 1959**, 145–173.

[13] Peng, C., Buldyrev, S., Havlin, S., Simons, M., Stanley, H., and Goldberger, A: Mosaic organization of DNA nucleotides. *Physical Review E* **49/2** (1994), 1685–1689.

[14] Weron, R.: Estimating long-range dependence: finite sample properties and confidence intervals. *Physica A* **312** (2002).